ISSN(Print): 1225-7672 / ISSN(Online): 2287-822X
DOI https://doi.org/10.11001/jksww.2018.32.5.381

Simulation of non-steady state oxygen transfer caused by microbubble supply

비정상상태의 미세기포에 의한 산소 전달 특성 모사

Jaiyeop Lee[1]·Ilho Kim[12*]
이재엽[1]·김일호[12*]

[1]*Department of Land, Water and Environment Research, Korea Institute of Civil Engineering and Building Technology (KICT), Gyeonggi-do, ilsanseo-gu, Goyangdae-ro 283, 10223*
[2]*Department of Construction Environment Engineering, University of Science and Technology, Daejeon, Yuseong-gu, Gajeong-ro, 217, 34113*
[1]한국건설기술연구원, 국토보전연구본부, 경기도 고양시 일산서구 고양대로 283, 10223
[2]과학기술연합대학원대학교, 건설환경공학부, 대전시 유성구 가정로 217, 34113

ABSTRACT

Microbubbles oxygen transfer to water was simulated based on experimental results obtained from the bubbles generation operated under varying liquid supply velocity to the multi-step orifices of the generator. It had been known that liquid supply velocity and bubble size are inversely related. In the oxygen transfer, a non-steady state was assumed and the pseudo stagnation caused the slow movement of bubbles from the bottom to the water surface. Two parameters were considered for the simulation: They represent a factor to correct the pseudo stagnation state and a scale which represented the amount of bubbles in supply versus time. The sum of absolute error determined by fitting regression to the experimental results was comparable to that of the American Society of Civil Engineers (ASCE) model, which is based on concentration differential as the driving force. Hence, considering the bubbles formation factors, the simulation process has the potential to be easily used for applications by introducing two parameters in the assumptions. Compared with the ASCE model, the simulation method reproduced the experimental results well by detailed conditions.

Key words: Micro-bubble, Oxygen transfer model, Non-steady state, Pseudo stagnation, Simulation

주제어: 미세기포, 산소전달모델, 비정상상태, 가-정체, 시뮬레이션

1. Introduction

The common macro size bubbles rise through water column rapidly and burst at the surface; whereas, microbubbles rise slowly and collapse under water. This and other physicochemical features of microbubbles cause a significant amount of gas dissolution and mass transfer to the water, subsequently making them applicable in variety of water and wastewater treatment processes (Agarwal et al., 2011; Burns et al., 1997; Khuntia et al., 2012; Li and Takahashi, 2014; Wen et al., 2011). The oxygen mass transfer to water solution in enhancing the dissolved oxygen concentration is basically described using Fick's diffusion law (Cussler et al., 1997).

The mass transfer is also clearly explained using mass transfer coefficients defined by the American Society of Civil Engineers (ASCE) standard (ASCE, 1984). Although

Received 18 July 2018, revised 13 September 2018, accepted 20 September 2018.
*Corresponding author: Ilho Kim (E-mail: ihkim@kict.re.kr)

a lot of improvements, mainly on the conversion methodologies from clean water to process water conditions, were incorporated into the 2006 version of ASCE standard, there is still a limitation in testing total dissolved solids content in water (Jiang, 2010). Therefore, the creation of a transfer model and simulation which considers the various influencing factors in a real transfer is required.

Most of the studies on modelling oxygen mass transfer as a function of time were developed on the basis of Fick's diffusion law. The species concentration gradient is the main driving force for the mass transfer and the control volume is divided by regions before and after boundaries (Ashley et al., 1991; Karamah et al., 2010). On the other hand, the transfer condition was determined by assuming an equilibrium around the bubble varying with time when Fick's law was developed. Worden and Bredwell (1998) assumed that the mass transfer of bubbles as a pseudo steady state. That is, through the slow increase in velocity, they assumed that the mass transfer approaches equilibrium uniformly with the surroundings. However, due to the continuous supply and the large number of bubble groups forming, constantly change.

The steady state is a simple transfer model widely used. But there is a limitation when the transferred mass affects to the concentration gradient. The unsteady state is the state that the transferred mass remains on surroundings, effecting the driving force in a form of gradient. It figures out the surrounding distribution of the concentration in the view of stagnant in short time. Therefore the unsteady state could be a proper description in stagnant transfer such as microbubble (Crank, 1965).

In this study, an unsteady state is assumed that the transfer results reflect continuously for the duration of the bubble's life span (Worden and Marshall, 1998). The life span was obtained from the convergence condition of the finite difference method and corrected as a factor, α. And the generated and supplied number of bubbles in groups was used as fitting parameter, β for regression with actual experimental results. To correct for the oxygen transfer process and introduce relevant parameters with the simulation results, a real-scale micro-bubble generator was designed and operated.

This methodology in simulating the processes would be built to figure the oxygen transfer process out definably as a white-box to apply to other fields widely. The process involved in this procedure would show the oxygen transfer step in a clear manner. Therefore, the bubble dissolving process was divided into each stage describing mass transfer. The results from the process using two factors could express the DO rising curve more precisely than the ACSE model.

2. Methodology

2.1 Simulation

2.1.1 Micro-bubble generation

In quantitatively describing the behavior of a bubble dissolving into water, the gas mass inside the initial bubble could be obtained from the ideal gas law (Eqn. 1).

$$n = pV/RT = p(4\pi r_s^3/3)/RT \quad (1)$$

where n is the quantity of matter inside a bubble, p is the equilibrium pressure, V is the bubble volume, R is the ideal gas constant, T is the temperature and r_s is the bubble radius. The pressure is obtained from hydrostatic pressure at the level of a bubble and surface tension. The surface tension could be obtained from Laplace-Young equation, Eqn. 2.

$$p = p_H + 2\sigma/r_s = (p_{atm} + \rho_w g z) + 2\rho/r_s \quad (2)$$

where p_H is the hydrostatic pressure, σ is the surface tension, p_{atm} is the atmosphere pressure, g is the gravitational acceleration, and z is the depth. r_s is referred to in Table 1, in which the supply liquid velocity of the gas-liquid mixture is related to the pressure value (Han et al., 2002). The size of the bubbles were analyzed by on-line particle counters (Chemtrac Model PC2400 D, USA).

Table 1. Estimated bubble size by liquid velocity in multi-step orifice (Han et al., 2002)

Pressure (atm)	2.0	2.5	3	3.5	4	4.5	5	5.5	6.0
Average size (μm)	71	54	41	30	28	28	29	31	28

2.1.2 Mass transfer

The generated bubbles transfer mass based on the concentration difference with the target solution. The mass transfer on interphase from gas to liquid was assumed to be governed and expressed by the diffusion coefficient (Worden and Bredwell, 1998). As the oxygen mass is transferred to the water solution, bubble size decreases. To simulate the transfer process, basically, the bubble was assumed to be spherical in shape (Brennen, 1995). Eqn. 3 gives Fick's law applied in a spherical axis.

$$\frac{\partial c_A}{\partial t} = -\frac{1}{r^2}\frac{\partial (N_A r^2)}{\partial r} = D\left(\frac{\partial^2 c_A}{\partial r^2} + \frac{2}{r}\frac{\partial c_A}{\partial r}\right) \quad (3)$$

C_A is the concentration of oxygen as a variable, t is time, r is the radius, N_A is the transfer flux, and D is the diffusion coefficient. When the left side is set to 0, the equation indicates a steady state. In this study, the modelling was conducted on the assumption that the atmosphere surrounding the bubble remained in a non-steady-state for as long as the bubble collapses. That is, the peculiar slow rise of a micro-bubble in the water column was regarded as a continuity of short stagnations. Hence, the non-steady-state around a bubble could be set by pseudo stagnation.

The non-steady state is a short moment scenario, so it is difficult to simulate a large number of bubbles. Therefore, we could use an algebraic expression of mass transfer for a spherical bubble introduced by Crank (1965), described in eqn. 4.

$$N_a'/4\pi r_s^2 = (c_{AO} - c_A)\frac{r_s}{3}\left[1 - \frac{6}{\pi^2}\sum_{n=1}^{\infty}\frac{1}{n^2}\exp\left(\frac{-Dn^2\pi^2 t}{r_s^2}\right)\right] \quad (4)$$

The transferred amount could be obtained from the flux, N_A', C_{A0} is the maximum saturation concentration, t is the time pseudo stagnation preserved. To obtain an appropriate initial value of t, the FDM(finite difference method) was set (eqn. 5).

$$\frac{c_A(r, t+\triangle t) - (c_A(r,t)}{\triangle t} = D\cdot\frac{1}{\triangle r^2}[c_A(r+\triangle r, t) - 2c_A(r,t) + c_A(r-\triangle r, t)] + D\cdot\frac{2}{r}\frac{c_A(r+\triangle r, t) - c_A(r,t)}{\triangle r} \quad (5)$$

Equation 5 could be rearranged to a differential equation, which is described eqn. 6.

$$c_A(r, t+\triangle t) = \triangle t\cdot D\cdot\frac{1}{\triangle r^2}[c_A(r+\triangle r, t) - 2c_A(r,t) + c_A(r-\triangle r, t)] + \triangle t\cdot D\cdot\frac{2}{r}\frac{c_A(r+\triangle r, t) - c_A(r,t)}{\triangle r} + c_A(r,t) = \left(1 - \frac{2D\triangle t}{(\triangle r)^2} - \frac{2D\triangle t}{r\triangle r}\right)\cdot c_A(r,t) + \left(\frac{D\triangle t}{(\triangle r)^2} + \frac{2D\triangle t}{r\triangle r}\right)\cdot c_A(r+\triangle r, t) + \frac{D\triangle t}{(\triangle r)^2}\cdot c_A(r-\triangle r, t) \quad (6)$$

To converge the differential equation, it was set the right side of the eqn. 6 to 1/2, the value of $\triangle r$, $\triangle v$ could be obtained. The obtained $\triangle t$ value, 2.9×10^{-x}, was then set as the boundary of the pseudo stagnation. To correct the stagnation time afterwards, a parameter, α, was introduced and used as a regression factor (eqn. 7).

$${}^{\alpha}N_A' = \alpha\cdot N_a' \quad (7)$$

2.1.3 Concentration change

When the water with bubbles was allowed to be continuously supplied, it was assumed that a regular amount is provided with time intervals. By this supply scheme, the transferred amount limited by pseudo stagnation was multiplied again by the cycled flux in a time step and the number in the suppled amount at a unit time. To represent this consideration, a parameter,

β, was included in the concentration term. On the other hand, the oxygen vapor pressure under continuous supply is in a different state than in an equilibrium; hence, the oxygen in solution is moved to air through the surface. Because this amount is proportional to C_A, the oxygen concentration in the solution after supply could be expressed by a constant factor, k, described in equation 8.

$$c_A = c_{AO} + \beta \cdot \alpha N_a{}' - k \cdot c_A \quad (8)$$

2.1.4 Bubble shrinkage

The mass amount inside a bubble varies due to mass transfer (Eqn. 9).

$$n_{i+1} = n_i - \alpha N_A{}' \quad (9)$$

n_{i+1} is mass remaining inside the bubble after mass transfer, and n_i is the mass in the previous step. The gap between the previous and the next step was set as the interval occurring transfer and could be inferred from the measured time gap in the experiment.

The variation of mass inside the bubble affects the pressure and size of the bubble and it was expressed by eqn. 10.

$$RT\triangle n = \triangle (pV) \approx V\triangle p + p\triangle V \quad (10)$$

$\triangle p$ was obtained from the pressure of the next step, p_{i+1}. But without the radius of the next step, $r_{s,\ i+1}$, we could not know the pressure. Furthermore, because the involvement of other variables is not yet clear, the trial radius value, $r_{p,}$ was replaced. By fixing p, we could obtain the change of the volume from the ideal gas equation (eqn. 11).

$$\frac{v_i}{n_i} = \frac{v_{i+1}}{n_i - \alpha n_A{}'} \quad (11)$$

The next step volume, V_{i+1} is a provisional volume obtainable by mass transfer. Here, r_p was obtained using eqn. 12.

$$r_p = \left(\frac{3}{4\pi} \cdot V_{i+1}\right)^{1/3} \quad (12)$$

By the time step, the height the bubble rises is reflected in $p_{H,\ i+1}$. The bubble vertical displacement, z, could be obtained from the rising velocity. $r_{s,\ i+1}$ is calculated from the final pressure.

2.1.5. Continual supply

Supplied bubbles shrink due to the mass transfer; while new bubbles are supplied by the continual inflow of generated micro-bubbles. Therefore, the defined time unit is the interval at which the new bubble group is fed. The newly supplied bubble group also is characterized by generation and shrinkage, just like the earlier supplied bubbles.

2.2 Experiment

2.2.1 Designation and operation of micro bubble generator

The micro-bubble generator process was designed for oxygen transfer with an operational property controlling the size of the bubble. The generator part was composed of a multi-step orifice structure to introduce mechanical pressure drop. The part volume was 30 L with a diameter of 0.3 m. The manufactured generator was tested on tap water to obtain an oxygen concentration (DO) transient plot which could be used as a regression parameter for simulation correction. Pure oxygen was used to prepare the gas-liquid mixture. The gas injection flow was fixed at 1.5 L/min. The gas was injected at the self-priming part with a diameter of 4 mm in the line. On the other hand, the liquid was supplied at velocities of 0.85 m/s, 1.02 m/s and 1.19 m/s, which correspond to pressures of 2.5, 3.5 and 4.5 atm, respectively, to induce bubble size change. These correspond with radii of 27, 15 and 14 μm, respectively (Table 1). The flow rate of the pump was 35 L/min. The saturation concentration was set at 33.31 mg/L for the 4.5 atm pressure. The values of DO were measured by Orion Star A223 RDO/DO meter (Thermo Scientific, USA) in the reactor with 200 L volume with a diameter of 0.6 m.

The set of the pressures, i.e., 2.5, 3.5 and 4.5 atm, which also could be expressed in the unit of flow, was

the adequate range and steps to generate microbubbles in this process considering the line diameter and the gas flow. Empirically, to generate microbubbles, the flow ratio of liquid to gas was set in the proportion of tens to one (Andinet et al., 2016). The ratio in this experiment *was* also in the range of 12.2~36.6.

2.2.2 Regression

The transient DO from the experiment was compared and used as a regression to fit with the result values to fit with the result values from the simulation structured by pseudo stagnation using parameter α and β. Optimal α and β values were obtained under the minimum sum of absolute error (SAE). The transient DO values obtained by regression were also compared with the values by the transfer model of ASCE.

3. Result and Discussion

3.1 DO transient model

The DO transient profile from the experiment, ASCE model and simulation were depicted for the cases of liquid velocity under 2.5, 3.5 and 4.5 atm in Fig. 1. The liquid velocity also gave definite results in the trend of mass transfer, as oxygen content (Worden et al., 1998). In the experiment, the DO increase tendency and saturated concentration values revealed differences under 2.5, 3.5 and 4.5 atm. An index expressing this profile qualitatively is the transfer coefficient k_La presented in the classical ASCE model. The simulation results were generally in agreement with the ASCE results, with slight differences in some aspects. In the plot of the experimental values, the whole transient profile displayed an inclining "S" shape. The curve from simulated values also showed a similar shape. In particular, values corresponding to the operating pressure of 2.5 atm displayed a clear fit to the experimental results. But, the ASCE model presented a parabolic curve, generally. The profiles by the ASCE model followed a similar tendency with the experimental results, but the initial drags in 0~600 seconds in DO increase did not fit well.

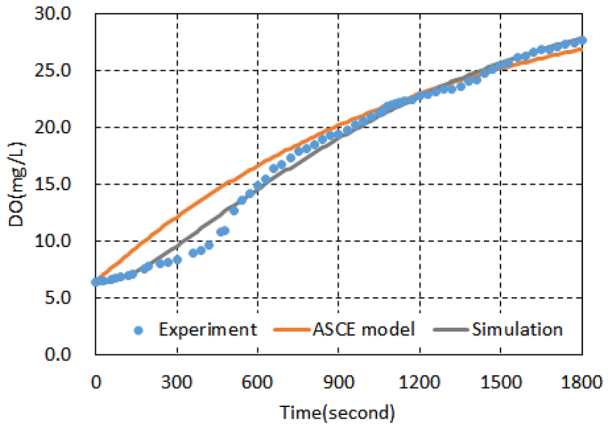

(a) 2.5 atm

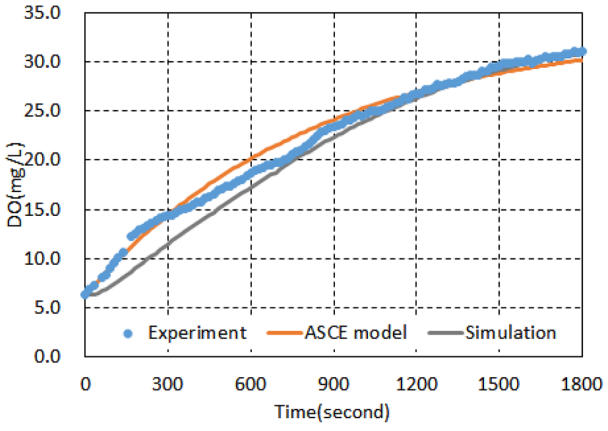

(b) 3.5 atm

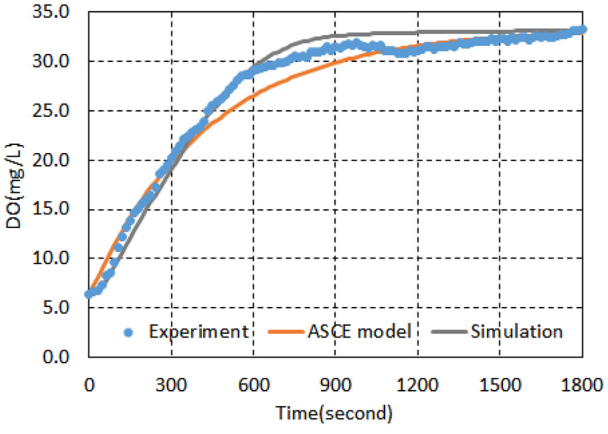

(c) 4.5 atm

Fig. 1. Transient DO variation by experiment, ASCE model and simulation based on liquid supply velocity.

The high DO concentration over 30 mg/L needs for the case that the already dissolved materials disturb the oxygen transfer or desirable for rapid improvement at anaerobic condition. Therefore the high concentration

would be necessary in wide-range field application. Using pure oxygen is efficiency and economical, saves operating cost (Andinet et al., 2016).

The correction parameters and transfer coefficients are given in Table 2. These values were obtained by regression of the experimental results. a, which indirectly expresses transfer period in a non-steady state, varied from 8.83 $\times 10^5$ to 3.54 $\times 10^6$. The higher the liquid velocity, the larger the value of a becomes. It was likely that the continuation of micro-bubble activity was caused by smaller bubble sizes. Thus, the pseudo stagnation state was affected by the proportion of small size bubbles.

β stands for the multiplied amount of the mass flux with the generated bubble number supplied per time. Its value ranged from 2.42 $\times 10^8$ to 3.99 $\times 10^9$ within the pressure range considered, which showed a significant increase. This is caused by longer stay periods and larger numbers of bubble generation with smaller size and larger supply inflow amounts according to the velocity. That is, β could be regarded as the index including generated bubble number and supplied amount, partially. On the other hand, k_La was from 8.0 to 23.0 ($\times 10^{-4}$) in proportion to liquid velocity. This also seemed to be a reflection of transfer potential by bubble size.

Table 2. The optimized values of α, β, KLa

Parameter		Pressure (atm)		
		2.5	3.5	4.5
Simulation	α	8.83×10^5	2.24×10^6	3.54×10^6
	β	2.42×10^8	1.45×10^9	3.99×10^9
ASCE	K_La	8.0×10^{-4}	1.2×10^{-3}	2.3×10^{-3}

To evaluate the reproducibility of the models, the sum of absolute error (SAE) is used. The SAE is the sum of the differences between the real experimental value, $x_{r,}$ and the estimated value, $x_{e,}$ as follows.

$$SAE = \sum |X_e - X_r|$$

SAE could be used as an index of agreement to experiment. The SAE for the simulation and ASCE models are given in Table 3. The simulation for the case of 2.5 atm best agreed with the experimental results, but the agreement became very weak under the remaining operating conditions. The case of 4.5 atm was almost in the same agreement for the two models. However, in the structuring detail transfer model, the ASCE model could not be established using these parameters, especially when the application was extended. Compared with the ASCE model, since the simulation method could reflect detailed conditions described in the methodology, it has an advantage when reproducing field applications.

Table 3. SAE of the simulation and ASCE model corresponding to pressure, in mg/L

Model	Pressure		
	2.5 atm	3.5 atm	4.5 atm
Simulation	30.1	129.0	116.4
ASCE	75.4	91.2	112.7

3.2 Shrinkage of bubble

Shrinkage of micro-bubble by transferring occurred as well in the simulation as in the reactor. In the model, the simulated process well depicted the size change of the bubble's radius as shown in Fig 2. We presumed that the bubble was not upraised by buoyancy drive. The disappearing times were over 1,800, 360 and 180 seconds, for 2.5 atm, 3.5 atm and 4.5 atm, respectively. By size, the equilibrium pressure between the inside and outside of bubble increased drastically according to the Laplace-Young equation. These differences make the shrinkage time gap between bubble sizes. Worden and Bredwell (1998) proposed that the micro-bubble's shrinkage occurs in 5 seconds. for pure oxygen for one bubble. Because this study employed massive amount of bubble group with half saturated DO concentration, the relatively long time for shrinkage could not be similarly comparable to previous works (Worden and Bredwell, 1998).

The flux to solution and mass change in a bubble is shown in Fig 3, respectively. The mass in a bubble was proportioned by the size, i.e. the volume. The amount of flux was proportioned by also mass possessed in the bubble, but the flux gradients at 3.5 and 4.5 atm were more precipitous in smaller size because of the

corresponding bigger pressure the bubble had.

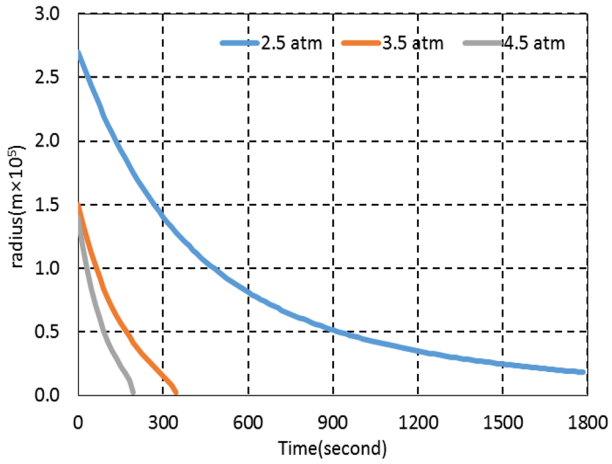

Fig. 2. Predicted shrinkage of micro-bubble in each experimental condition by simulation.

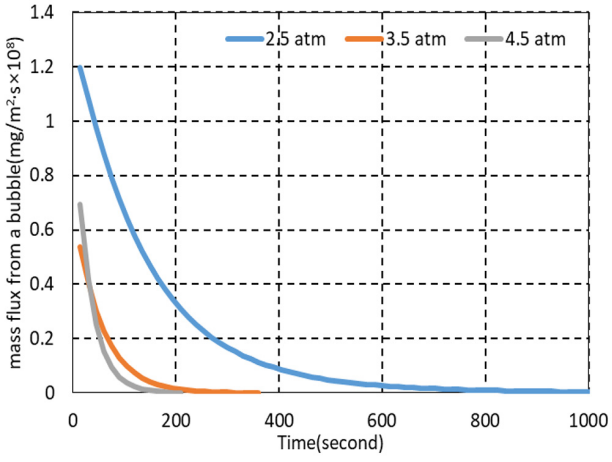

(a) Mass flux

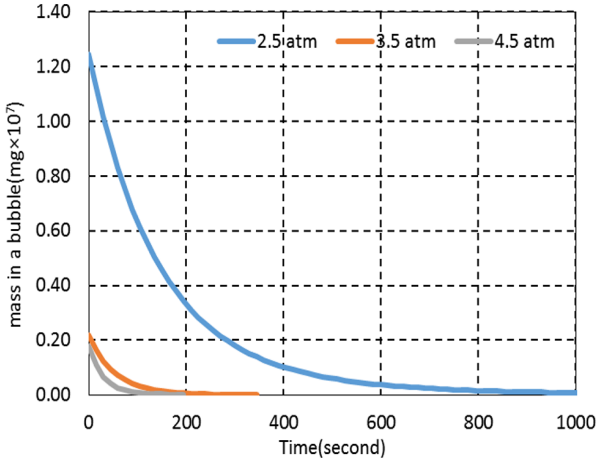

(b) Mass change

Fig. 3. Predicted flux outside and mass change in micro-bubble condition by simulation.

4. Conclusions

In this study, a mass transfer model was structured assuming spherically shaped bubble diffusion under a non-steady-state brought about by pseudo stagnation. Using the model, micro-bubbles dissolved oxygen transfer to water solution was quantified. In the experiment, the bubble size was controlled by varying liquid supply velocity, which was reflected in the models. In the modelling, a and β were selected as fitting parameters for the experimental results, representing corrected stagnation time and bubble amount with cycles in time step, respectively. The structured model well simulated the real experimental results, except for the initial drag shape that showed variation in dissolved oxygen. The result was also compared with that of the ASCE model, which is a simple model having a transfer coefficient. The averaged SAE of the simulation was 91.8, which was slightly lower than that of ASCE. Assuming pseudo stagnation, parameters a and β varied 8.83×10^5~3.54×10^6 and 2.42×10^8~3.99×10^9, respectively. The structured model was able to reflect the various factors in bubble generating conditions. This gives an applicability of the model extension by experimental values or the conditions change of microbubble generation such as various field.

References

Agarwal, A., Ng, W.J. and Liu., Y. (2011). Principle and applications of microbubble and nanobubble technology for water treatment, Chemosphere, 84, 1175-1180.

Andinet, T., Kim, I. and Lee, J. (2016). Effect of microbubble generator operating parameters on oxygen transfer efficiency in water, Desalination Water Treat., 57, 26327-26335.

ASCE (1984). ASCE Standard: Measurement of Oxygen Transfer in Clean Water, American Society of Civil Engineers, New York, NY.

Ashley, K.I., Hall, K.J. and Mavinic, D.S. (1991). Factors influencing oxygen transfer in fine pore diffused

aeration, Water Res., 25, 1479-1486.
Brennen, C.E. (1995). Cavitation and bubble dynamics. Chapter 2: Spherical bubble dynamics, Oxford University Press, 48-78.
Burns, S.E., Yiacoumi, S. and Tsouris, C. (1997). Microbubble generation for environmental and industrial separations, Sep. Purif. Technol., 11, 221-232.
Cussler, E.L. (1997). Diffusion, mass transfer in fluid systems. Chapter 8, Fundamentals of mass transfer. Second ed., Cambridge university press, 237-273.
Crank, J. (1965). The mathematics of diffusion, 2nd Eds., Clarendon Press, Oxford, 89-103.
Jiang, P. (2010). Gas transfer parameter estimation: applications and implications of classical assumptions. PhD dissertation, University of California, Los Angeles.
Karamah, E.F., Bismo, S., Annasari, L. and Purwanto, W.W. (2010). Mass transfer study on micro-bubbles ozonation in a bubble column, Int. J. Chem. Eng. Res., 2(2), 243-252.
Khuntia, S., Majumder, S. K. Ghosh, P. (2012). Microbubble-aided water and wastewater purification: A review, Rev. Chem. Eng., 28(4-6), 191-221.
Li, P. and Takahashi, M. (2014). Applications of microbubbles in the field of water and wastewater treatment. In: H. Tsuge (Ed.), Micro- and nanobubbles, fundamentals and applications, Pan Stanford Publishing, USA.
Han, M., Park, Y., Lee, J. and Shim, J. (2002), Effect of pressure on bubble size in dissolved air flotation, Water Sci. Technol., 2(5-6), 41-46.
Wen, L.H. Ismail, A.B. Menon, P.M. Saththasivam, J. Thu, K. and Choon, N.K. (2011). Case studies of microbubbles in wastewater treatment, Desalination Water Treat., 30, 10-16.
Worden, R.M., Bredwell, M.D. (1998), Mass-transfer properties of microbubbles. 2. Analysis using a dynamic model, Biotechnol. Prog., 14(1), 39-46.